How does the water springtail optically locate proper habitats? Spectral sensitivity of photo- and polarotaxis in *Podura aquatica*

Ádám Egri[1,2,*] and György Kriska[1,2,3]

1: Danube Research Institute, MTA Centre for Ecological Research,
H-1113 Budapest, Karolina út 29-31, Hungary

2: Evolutionary Systems Research Group, Centre for Ecological Research, Hungarian
Academy of Sciences, Klebelsberg Kuno u. 3, H-8237 Tihany, Hungary

3: Group for Methodology in Biology Teaching, Biological Institute, Eötvös University,
H-1117 Budapest, Pázmány sétány 1, Hungary

*Corresponding author, e-mail address: egri.adam@okolologia.mta.hu

ABSTRACT

Optical water detection by means of horizontally polarized light is widespread among aquatic insects. This ability of these insects usually works in the UV or blue spectral ranges. Recently it was demonstrated that at least one collembolan species, the water springtail (*Podura aquatica*) also possess positive polarotaxis to horizontally polarized light. These hexapods are positively phototactic, live on the surface of calm waters and usually accumulate in the intimate vicinity of the riparian vegetation. In laboratory experiments we measured the wavelength dependence of phototaxis and polarotaxis of *P. aquatica* in the 346 nm − 744 nm and 421 nm − 744 nm ranges, respectively. According to our results, the action spectrum of phototaxis is bimodal with two peaks in the blue ($\lambda_1 = 484$ nm) and green-yellow ($\lambda_2 = 570$ nm) ranges, while polarotaxis operates in the blue spectral range. For the first time we have shown that collembolan polarotaxis functions in the same spectral range as the polarotaxis of many aquatic insects. In this paper we present our experiments and discuss the possible ecological significance of our findings.

Key words: Collembola, *Podura aquatica*, polarization vision, phototaxis, polarotaxis, visual ecology

INTRODUCTION

Springtails (Collembola) are tiny arthropods playing essential role in terrestrial ecosystems by contributing to the decomposition of organic matter. At the moment approximately 7000 species are known, but at least 50 000 species are estimated to be present on our planet (Hopkin, 1997). They inhabit all types of terrestrial habitats including the most extreme places like deserts, polar regions and the highest mountains (Hopkin, 1997). Nearly all of the springtails feed on decaying plant material and fungi (Rusek, 1988), although a few species have been reported to feed on live plants (Hopkin, 1997; Bishop et al., 1998). Collembola species are usually negatively phototactic (Salmon and Ponge, 1998; Fox et al., 2007) and live in the soil or in its uppermost layer. Contrary to the majority of springails the water-surface-inhabiting *Podura aquatica* (Linnaeus, 1758) is positively phototactic, like other species living on plants or on the surface of water (Shaller, 1972). Contrary to desert-inhabiting springtails *P. aquatica* is extremely sensitive to desiccation, thus water intake must happen almost constantly, which is usually performed via a specialized organ, the ventral tube (Noble-Nesbitt, 1963). When undisturbed, these dark bodied springtails congregate at the surface of ponds or very slowly moving waters close to the shore and the riparian vegetation (Verheijen and Brouwer, 1971; Childs, 1915) (Fig. 1). In the case of an approaching object they perform several-centimeter-jumps with the help of their fork shaped locomotory organ, the furcula.

Although, most of the springtails possess eyes, the known species has no more than only eight ommatidia per eye, which is also the case for *P. aquatica*. Moreover, due to the high acceptance angles of these ommatidia (up to 80°), their field of view usually overlap thus the resolution of collembolan eyes is very low (Shaller, 1972).

Numerous aquatic insects recognize water surfaces optically by means of the water-reflected horizontally polarized light (Schwind, 1983, 1984, 1989, 1991, 1995; Wildermuth, 1998; Horváth and Varjú, 2004; Csabai et al., 2006; Horváth et al., 2008). Recently, as the first example for a Collembola species, we have demonstrated that *P. aquatica* also possess positive polarotaxis to horizontally polarized light (Egri et al., 2016). Now our primary aim was to study the wavelength dependence of the photo- and polarotaxis of *P. aquatica*. In this study we present the results of laboratory choice experiments and we discuss how the spectral and reflection polarization characteristics of the environment may synergistically determine the habitat selection of *P. aquatica*.

MATERIALS AND METHODS

Springtails

Female and male adult *P. aquatica* were collected from the surface of ponds near Budapest (47° 36' 37.29" N, 19° 7' 24.24" E, Fig. 1) and were kept at 13°C under 12 h:12 h dark:light conditions in plastic containers with pond-water, duckweed and other plant leaves collected from the same site. Diffuse light of a cool white LED lamp was used for lighting the containers. The emission spectrum of this illumination was measured with a radiometrically calibrated, cosine corrector (CC-3-UV-S) equipped Ocean Optics STS-VIS spectrometer (Ocean Optics, Largo, USA) (Fig. S1A). Based on this measurement the total photon flux of this illumination was 1.47×10^{14} photons·cm^{-2}·s^{-1}). Animals were kept in captivity no more than 5 days long before experimenting.

Light source

In the experiments a custom built, Arduino UNO controlled light source was used which contained 14 power LEDs covering the 346 nm – 744 nm spectral range (Fig. 2). A Moritex SOHC4S3.5-1500S four-branch quartz light-guide was used to deliver the light stimuli to the springtails. The LEDs were fixed on a two dimensional motorized stage in a box. To emit the light of the desired LED into the light-guide, the stage was moved to the proper position. The intensity of light at the light-guide outputs was controlled electronically and also with neutral density filters: (i) The currently selected LED's light intensity was controlled with pulse width modulation (Barr, 2001) signal with a frequency of $f_{PWM} = 980$ Hz, and a (ii) filter wheel was also applied between the light-guide and the LEDs mounted on the motorized stage. The filter wheel had 4 windows: The first window was empty, the second, third and fourth contained

one, two and three pairs of Lee 210 and Lee 211 (LEE Filters, Andover, UK) neutral density filters respectively (Fig. S1B). With the combination of these two intensity controlling methods the light intensity of the different monochromatic stimuli was variable through several log intensity units depending on the wavelength. The light intensity of each LED in the light source was calibrated with the previously mentioned Ocean Optics STS-VIS spectrometer through empty space, and the transmission spectra of the neutral density filters in the filter wheel were also measured (Fig. S1B). With mathematical combination of these information the light intensity of any stimulus could be calculated for a given PWM signal. The measurement range of the spectrometer allowed us to calibrate only 13 out of the 14 monochromatic LEDs. The shortest wavelength LED (CUD4AF1B, λ = 346 nm, Seoul Viosys, Seoul, Republic of Korea) was calibrated with an OPT101 photodiode based on the photodiode's spectral sensitivity curve, and the shape of the LED's emission spectrum both available in the corresponding datasheets. The exact type of the other power LEDs were unknown, but it is not a problem because their emission spectrum was exactly measured. Figure 2 shows the normalized emission spectrum of each LED measured at the light-guide outputs. Throughout this study light intensities of stimuli in the experiments and measured emission spectra were calibrated for photon numbers.

In addition to the calibration of the light source we checked if the angular distribution of light exiting the light-guide outputs were similar. We pointed one light-guide output to a white paper perpendicularly from 14 cm. For each wavelength the other side of the paper was photographed in RAW image format with a NIKON D3200 DSLR camera. The intensity along the diameter of the light spot was plotted, a Gaussian function was fitted on each measurement and full-width half-maximums (FWHM) were calculated (Fig. S2). The high noise in Supplemetary Figure S2N occurred because the light of the longest-wavelength-LED (744 nm) was almost invisible for the camera. The FWHM for the light-guide outputs were α_1 = 21.63° ± 1.35°, α_2 = 22.91° ± 1.43°, α_3 = 22.86° ± 1.32°, and α_4 = 22.02° ± 1.55° (mean ± standard deviation) thus the angular distribution of the stimuli of each output was quite similar.

Experiment 1 – Action spectrum of phototaxis

The wavelength dependence of positive phototaxis of *P. aquatica* was measured in the 346 nm – 744 nm range at 14 different wavelengths in a darkened chest lined with black material. Springtails were tested in a 86 mm × 26 mm × 1 mm (length × width × height) rectangular arena composed of black cardboard. Three pieces of 1 mm thick 30 mm × 30 mm quartz glasses were used for covering the arena to prevent the escape of the springtails and to allow their observation and stimulation with light. Stimulation was performed with the previously described light source using all 4 outputs of the light-guide in parallel: Light-guide outputs were directed onto one end of the arena from 60° measured from the horizontal thus when light stimulus was delivered on the springtails, they could move in a light gradient. A 3 mm sandblasted glass was placed between the light-guide and the arena to act as a diffuser to ensure a smooth light gradient in the arena. The transmission spectrum of the quartz and sandblasted glass were taken into account when a light stimulus was applied (Fig. S1B). The movement of springtails in the arena was recorded by a Genius WideCam F100 USB webcam modified for infrared sensitivity. The arena was illuminated from above by an SMD5050-150-IR infrared LED strip (length = 30 cm) having emission peak at 940 nm. Springtails were detected with an algorithm adapted from Egri et al. (2016).

During trials the relative humidity, which was measured with a HIH-4000 Series humidity sensor, varied between 50% and 55%. Since *P. aquatica* is extremely sensitive for low humidity as other Collembola species, too much time in the arena would have been lethal for the tested springtails and would have produced false results. Based on preliminary tests we found that the first 15-20 minutes were not stressful for them and they were moving constantly, but thereafter we observed decrease in their activity and after 50 minutes only 20% of them was moving. For this reason we could not allow very long dark adaptation times before each light stimulus.

In each trial one wavelength was tested as follows: 20-35 specimens were placed in the arena where they could freely walk, but could not jump. After 3 minutes of dark adaptation the test started by applying 30-second-long light stimuli separated with 60-second-long dark periods. Except for 744 nm, all together 6 light stimuli were applied in a given trial with logarithmically increasing light intensity. This was due to the increased transmission of the neutral density filters above 700 nm (Fig. S1B), which did not allow us to set the initial light intensity as low as for the other wavelengths. The purpose of the dark periods was two fold. Besides the need of dark adaptation, the springtails had to be given the opportunity to distribute randomly before the next stimulus. For measuring the springtail attraction to light in

case of a given light intensity and wavelength we calculated their relative centroid shift Δx towards the illuminated side of the arena at the end of the stimulus measured from the arena center. Here we call this shift relative because it was measured in arena-length-units. The implementation of the trials and the evaluation process is demonstrated by Supplementary Video M1. In this experiment n=10 trials were performed for each wavelength and all together 3613 *P. aquatica* were tested. To test if a given light stimulus elicited significant response, we applied Mann-Whitney U test for comparing the distribution of responses (Δx at the end of stimulus) with the distribution of Δx values at the beginning of the given stimulus.

The action spectrum of phototaxis was obtained very similarly as described in Mazza et al. (2010). Mean responses (Δx) of springtails were plotted as a function of the logarithm of stimulus intensity $J = \log(I_{stimulus})$ for all wavelengths the following sigmoid dose-response curve was fitted on these mean responses with Gnuplot v5.2 (http://www.gnuplot.info):

$$f(x) = A_1 + (A_2 - A_1) \cdot (1 + \exp((J - J_{50\%})/s))^{-1} \qquad (1)$$

A_1 and A_2 are the two extremal values of the curve, $J_{50\%}$ is the logarithm of light intensity $I_{50\%}$ corresponding to 50% response and s is related to the steepness of the curve. We applied $A_2 = 0$ for fitting because in the case of $I_{stimulus} = 0$ the expected Δx value was zero. Thus for each wavelength $I_{50\%}$ is the light intensity required for eliciting half of the maximal response. The action spectrum was calculated by obtaining the reciprocals of these intensities as a function of wavelength, then normalizing the curve with the maximal value. The uncertainty of the points of the action spectrum was obtained from the asymptotic standard error of the fitted $J_{50\%}$ parameters. Cubic spline interpolation was used to locate the maxima of the action spectrum.

Experiment 2 – Action spectrum of polarotaxis I

We have performed choice experiments with *P. aquatica* to test their preference for horizontally polarized light over vertically and unpolarized light as a function of wavelength in the 421 nm – 744 nm range including 11 different wavelengths. The choice-arena was a linear, two-window arena (length = 30 cm, width = 10 cm, height = 6.5 cm) where the springtails started to move towards the preferred light stimulus from the center. The stimulus windows were composed of 7.1 cm × 5.7 cm sandblasted glass (width = 3 mm) and the inner surface of the arena was covered with matte white paper for minimizing polarization-related disturbances. Before each test a new piece of white paper was used as bottom to minimize

odour clues from the previously tested springtails. The light stimuli were created with the same light source as described above, but by using 2 outputs of the light-guide per stimulus window of the arena. The light from the light-guide outputs was diffused by a creased aluminium foil reflector symmetrically on each side of the arena. With this experimental arrangement equal-intensity stimulus pairs could be delivered into the arena across the two windows. The tests were performed in the same darkened chest as experiment 1, and the same infrared-camera-method was applied for recording the springtails (Fig. 4).

Before each trial the desired stimulus pair was set, then 80-150 *P. aquatica* specimens were placed into a standing plastic releaser tube (diameter = 28 cm) at the center of the arena. After 30 s the releaser was removed and the chest was quickly closed. During the following 110 s, images were saved by the camera every second. Later, all of the photographs were evaluated with the method of Egri et al. (2016), thus the number of springtails at the left, middle and right third of the arena and the relative centroid shift Δx has been obtained as a function of time. For each trial these values were averaged in the 80 s − 110 s interval. For example, regarding the relative centroid shift of the springtails, Δx was considered as the mean of the measured Δx values during the last 30 s of the given trial. The same principle was applied for the determination of the springtail numbers in the left, middle and right thirds of the arena. Numbers of choices were considered as numbers of springtails in the left or right third of the arena, while numbers of specimens in the middle third of the arena were treated as numbers of inactive individuals that did not choose stimulus. With this method the track of animals could not be determined because the springtails usually performed jumps during the tests. The animals could not jump out from the arena, but at the sides they could get under the paper lining on the bottom, thus a slight decrease in their numbers may occurred, but it was negligible. Supplementary video M2 summarizes the evaluation method of the trials of experiments 2 and 3.

In experiment 2 we tested the preference of *P. aquatica* for horizontally polarized versus unpolarized stimuli. In the case of real positive polarotaxis a highly polarized light stimulus is more attractive than an unpolarized stimulus with the same emission spectrum even if the polarized light's intensity is two or more times lower (Egri et al., 2016). Since *P. aquatica* is positively polarotactic to horizontally polarized white light (Egri et al., 2016), one of the best strategies to test the wavelength dependence of polarotaxis was to use horizontally polarized and unpolarized stimulus pairs with at least two times dimmer light stimulus on the polarized side. Hence, polarized stimuli were created by inserting a visual-range linear polarizer (XP42-18, ITOS, Mainz, Germany) between the aluminium reflector and the

window of the arena with horizontal transmission axis (Fig. 4D). This arrangement inherently produced an approximately 60% dimmer polarized stimulus than the unpolarized stimulus with no polarizer. The photon flux of the unpolarized stimuli was 8.6×10^{12} photons·cm^{-2}·s^{-1}. Table 1 summarizes the relative light intensities of polarized stimuli compared to the corresponding unpolarized stimulus (no polarizer) as a function of wavelength calculated from the emission spectra of the unpolarized stimuli and the transmission spectrum of the polarizer. In case of visible wavelengths the degree of polarization d of stimuli was measured by imaging polarimetry (Horváth and Varjú, 1997, 2004, Egri et al., 2016), and the results showed that d was practically constant across the applied wavelengths (Table 1). Because the emission spectrum of the stimuli were narrow peaks (Fig. 2), the polarized and unpolarized stimuli had practically the same emission spectrum.

For each stimulus pair 4 trials were performed, 2 with swapped stimuli in order to compensate for incidental asymmetries of the setup. We plotted the total numbers of choices and mean centroid shifts towards horizontally polarized stimulus (Δx) as a function of wavelength. For estimating the wavelength of maximal polarotaxis we fitted a Gaussian function on the Δx points corresponding to the positive-polarotaxis-reactions. To check the significance of total choice numbers for a given wavelength, χ^2 tests were applied: Taking into account the corresponding 4 trials, total number of springtails choosing horizontally polarized stimulus were compared with total number of specimens choosing the unpolarized side.

Experiment 3 – Action spectrum of polarotaxis II

According to Egri et al. (2016), for a given emission spectrum, the most, moderately and less attractive light for *P. aquatica* are horizontally polarized, unpolarized and vertically polarized, respectively. Thus, for a given wavelength, the most striking reaction could be achieved by a horizontally/vertically polarized stimulus pair. For this reason, in experiment 3 we have also performed trials with horizontally and vertically polarized stimuli by applying polarizers at both sides of the arena. Consequently, in these trials the light intensities of the stimuli were equal. In this experiment the total number of springtails choosing horizontally and vertically polarized stimulus were compared with χ^2 tests in case of all tested wavelengths (Table 1).

Spectral characteristics of the habitats of *P. aquatica*

At our springtail collecting site several small lakes and ponds are located where *P. aquatica* is abundant. At one of these water bodies we have measured the spectral characteristics of the environment from the aspect of a springtail standing on the water in the vicinity of the riparian vegetation. Spectral acquisitions were performed with the same Ocean Optics STS-VIS spectrometer mentioned before. With the help of a small spirit level the cosine corrector (acceptance angle = 180°) of the spectrometer was positioned 4 cm above the water surface with horizontal optical axis. Measurements were performed from a fishing pier (i) towards the open water and (ii) towards the bank. During the measurements the spectrometer was 80 cm from the vegetation (reed) at the bank of the small lake. Measurements to both directions were done 4-4 times under sunny and total overcast conditions during moderate solar elevation. The aim of these measurements was to get spectral information about the summed, global light coming from the side of open water and the riparian zone at the position of a hypothetical springtail standing on the water in the vicinity of the shore.

Additional methodological and analytical information

(i) *P. aquatica* is not protected in Hungary, thus no permission was needed for our experiments. (ii) Human subjects were not involved in our study. (iii) No reagents were used.

RESULTS

Figure 5 demonstrates the average responses of springtails as a function of light intensity for all 14 wavelengths with asterisks indicating if the given stimulus was significant ($p < 0.05$), according to the Mann-Whitney U test. Figure 6 shows the action spectrum of phototaxis of *P. aquatica* as a function of wavelength in the 346 nm – 744 nm spectral range calculated from the sigmoid dose-response curves fitted on the points of Fig. 5. The action spectrum of phototaxis is mostly restricted to the visible range, and is bimodal with peaks at wavelengths $\lambda_1 = 484$ nm and $\lambda_2 = 570$ nm. In other words, the phototaxis of *P. aquatica* has two peaks, one in the blue and one in the yellowish-green ranges of human vision (Fig. 6). This is the reason why a visible-range polarizer was sufficient for the polarotaxis experiments (exps. 2 and 3), however there was a little but significant phototaxis below the λ_1 peak.

Figure 7 demonstrates the responses of springtails for horizontally polarized/unpolarized stimulus pairs as a function of wavelength in the spectral range of 421 nm – 744 nm. In Fig. 7A the proportion of total springtail choices are shown for each wavelength. Black and grey bars represent the proportion of choices in the horizontally polarized and unpolarized side of the arena respectively, while grey bars indicate the proportion of inactive specimens that stayed in the middle third of the arena. In case of all wavelengths the total numbers of tested springtails ($N_{polarized} + N_{middle} + N_{unpolarized}$) are shown by numbers in the gray bars. Asterisks show the significance of χ^2 tests calculated from the total number of choices obtained in the two sides of the arena ($N_{polarized}$ versus $N_{unpolarized}$). The means of relative centroid shifts (Δx) of the 4 trials are plotted in Fig. 7B as a function of wavelength with vertical bars denoting standard errors.

According to Fig. 7, in experiment 2 the dimmer horizontally polarized light (Table 1) was more attractive than the unpolarized stimulus at three neighboring wavelengths between 467 nm and 516 nm. Thus this was the range of positive polarotaxis for horizontally polarized light. Gaussian fitting revealed that the maximal polarotactic reaction corresponds to $\lambda_{exp2} = 491$ nm. On both sides of this peak phototaxis overwhelmed polarotaxis and the unpolarized stimulus was more attractive than the horizontally polarized one. Regarding the wavelengths over 641 nm no significant preference could be observed.

Figure 8 shows the responses of *P. aquatica* in experiment 3 for equal-intensity stimulus pairs of horizontally and vertically polarized light with the same concept as Fig. 7. The shape of the bar plot and the curve in Fig. 8 is qualitatively similar to that of Fig. 7. Horizontally polarized light was significantly more attractive for the springtails than the vertically polarized stimulus again in the range of 467 nm – 516 nm. It is also clear that the magnitude of polarotactic reactions were higher in experiment 3 (Fig. 8) than in experiment 2 (Fig. 7), which is not surprising because the horizontally-vertically polarized stimulus pair elicits the most striking reactions (Egri et al. 2016). In the case of experiment 3 the wavelength of maximal attraction to horizontally polarized light was $\lambda_{exp3} = 492$ nm.

The results of spectral measurements of the habitat of *P. aquatica* are shown in Fig 9. Figure 9A demonstrates the panorama photograph of the scene where the spectral measurements were performed. Thick blue and green arrows represent the horizontal direction of the optical axis of the spectrometer's cosine corrector in the case of the measurements towards the open water and bank side respectively. Figures 9B and C indicate the mean measured spectra when the weather was sunny and overcast respectively, thus each curve is an average of 4 measurements. We worked with spectra measured in photon units rather than

power units, because biological processes depend on the number of absorbed photons (Johnsen, 2012). In Figs 9B and C the FWHM of the two peaks of the action spectrum of phototaxis (Fig 6.) are shown with grey regions. To estimate the ratio of phototaxis-eliciting short ($\sim\lambda_1$) and long ($\sim\lambda_2$) wavelength photons we integrated the spectra in the FWHM regions of the action spectrum of phototaxis and divided them with each other (Figs 9B-C). It is clear from these graphs, that independent of the weather conditions, in this model the behaviour-influencing light intensity around λ_1 was relatively higher than around λ_2 in the case of the open water side (blue curve) than in the case of the bank side (green curve). In other words, from the aspect of a *P. aquatica* specimen the bank side had more long wavelength components than the side of open water independent of the cloud coverage. It is also clear that the light intensities were lower in most wavelengths towards the bank, because towards the open water the brighter skylight was more dominant.

DISCUSSION

Spectral sensitivity of insects usually ranges from the UV to the green regions of the spectrum, although some butterfly species posses receptors with absorption maximum in the red channel (Menzel and Backhaus, 1991; Briscoe and Chittka, 2001). As Fig. 6 shows, the phototaxis of *P. aquatica* is restricted to the blue-green-yellow range with two peaks ($\lambda_1 = 484$ nm and $\lambda_2 = 570$ nm). According to the results of experiments 2 and 3 (Figs 7-8), there were spectral regions where (i) polarotaxis dominated, (ii) simply phototaxis occurred or (iii) no preference was recorded. Polarotaxis was observed in a narrow spectral region in the blue range (Figs 7 and 8). In Figs 7 and 8 it is also shown that spectral regions where phototaxis overwhelmed the attraction to horizontally polarized light occurred on both sides of the shorter wavelength peak (λ_1) of the action spectrum of phototaxis (Fig. 6). In Fig. 6 a slight increase can bee seen towards the UV range, but our measurement range do not allow us to make a judgement if there is really another peak of phototaxis in the UV range. Light stimuli with wavelengths above 641 nm did not elicit any significant reactions in the experiments. This is also shown by the low choice numbers for these long wavelengths in Figs 7A and 8A. Low choice numbers compared to the numbers of inactive individuals indicate that the springtails did not perceive well the red–infrared stimuli. Although the polarization characteristics of the stimuli at the arena terminals were different, the majority of the springtails stayed in the middle third of the arena, because such long wavelengths were sensed as darkness. This is not surprising, because insects usually lack red-sensitive photoreceptors (Menzel and Backhaus, 1991).

Based on these results we suggest that *P. aquatica* possess at least two different visual pigments, however it should be tested with absorption spectroscopy or electroretinography, but the latter is extremely difficult task for such tiny and vulnerable animals. What we can unambiguously conclude is that polarotaxis *of P. aquatica* functions in the blue spectral range peaking between 484 nm and 492 nm, and longer wavelengths, particularly around $\lambda_2 = 570$ nm, are also perceived well by this species but this range plays role only in phototactic behaviour. In the nature there is no situation when the global illumination is monochromatic, because the Sun is a black body radiator, thus it has a broad emission spectrum (Cronin et al., 2014). Consequently, in a terrestrial natural habitat the light scattered from the sky or returned from field objects (e.g. water, plants, rocks, soil) will usually contain most wavelengths of the Sun's global illumination, but the spectral composition can change depending on the absorption and reflection spectrum of these objects. Our spectral measurements of the habitats of *P. aquatica* (Fig. 9) were performed via a cosine corrector with hemispherical field of view. This method was suitable only for collectively measuring the spectrum of all lights coming from the direction of the shore or the open water. Although we do not know exactly what kind of image forms in the visual system of *P. aquatica*, it is clear that the measured irradiances (Fig. 9) towards the shore contain relatively more long-wavelength ($\sim\lambda_2$) components compared to the short-wavelength components ($\sim\lambda_1$). However it is trivial, since every amateur and professional naturalist knows that field objects in the nature are commonly greenish, yellowish or brownish, but towards the open waters the spectral composition of the blue or cloudy sky dominates. It is a common observation that *P. aquatica* usually avoid open waters and accumulate in the intimate vicinity of the shore, where decaying and living plant materials are usually present (Verheijen and Brouwer, 1971; Childs, 1915) (Fig. 1). We suggest that the second peak of the action spectrum (λ_2 in Fig. 6) serves the discrimination of the riparian zone from the open water, however, it should be tested in further experiments.

In aquatic insects the polarization sensitivity operates usually in the short-wavelength spectral range, mainly in the UV or blue (Schwind, 1991, 1995). It has been explained as an adaptation to the optical environment since in the nature the degree of polarization of water-reflected light increases with decreasing wavelength (Schwind, 1995; Horváth and Varjú, 1997). Based on our results *P. aquatica* possess the same ability with its blue-sensitive positive polarotaxis. To mention another example for spectral adaptation of polarotaxis, Flamarique and Browman (2000) demonstrated that two *Daphnia* species utilize middle-wavelength pigments for polarization vision which wavelength range is more common underwater in lakes and ponds which are the habitats of these planktonic crustaceans. For *P.*

aquatica the ability of polarization vision may not only be important for maintaining position on the water surface or in the intimate vicinity of water bodies. According to Childs (1915), this species burrow into the mud close to the shores when winter is approaching and they return to the water surfaces in the beginning of spring. Thus polarization vision may also play role in water-seeking of *P. aquatica* right after the dormant state, however it has been also claimed that *P. aquatica* overwinter under the water level (Heckman, 2018).

The main message of our study is that similarly to a variety of aquatic insects the polarotaxis of *P. aquatica* functions in the blue spectral range, but, longer-wavelength light is also important for this species. Polarotaxis serves water detection and phototaxis may play role in the recognition of the riparian zone. With this strategy the low-resolution-eyed water springtail can easily find visually the safest and food-rich habitats, which are water surfaces surrounded by vegetation. In the present paper we suggested that the optical habitat selection of *P. aquatica* is relying both on the reflection-polarization and spectral characteristics of their visual environment.

ACKNOWLEDGEMENTS

COMPETING INTERESTS
The authors declare no competing or financial interests.

REFERENCES

Barr, M. (2001). Pulse width modulation. *Embedded Systems Programming* **14**, 103–104.

Bishop, A. L. M., McKenzie, H. J., Barchia, I. M. and Spohr, L. J. (1998). Efficacy of insecticides against the lucerne flea, Sminthurus viridis (L.) (Collembola: Sminthuridae), and other arthropods in lucerne. *Aust. J. Entomol*. **37**, 40–48.

Briscoe, A. D. and Chittka, L. (2001). The Evolution of Color Vision in Insects. *Annu. Rev. Entomol.* **46**, 471–510.

Csabai, Z., Boda, P., Berná th, B., Kriska, G. and Horváth, G. (2006). A 'polarisation sun-dial' dictates the optimal time of day for dispersal by flying aquatic insects. *Freshwater Biol.* **51**, 1341–1350.

Childs, G. H. (1915). Some Observations on the Life History of the Water Springtail (Podura Aquatica-1758). Thesis submitted to the Faculty of the Graduate School of the University of Minnesota, May 25 1915, p.1–63.

Cronin, T. W., Johnsen, S., Marshall, N. J. and Warrant, E. J. (2014). *Visual Ecology*. Princeton: Princeton University Press.

Egri Á., Farkas A., Kriska G. and Horváth G. (2016) Polarization sensitivity in Collembola: an experimental study of polarotaxis in the water-surface-inhabiting springtail *Podura aquatica*. *The Journal of Experimental Biology* 219, 2567–2576.

Flamarique, I. and Browman, H. I. (2000). Wavelength-dependent polarization orientation in Daphnia. *Journal of Comparative Physiology A: Sensory, Neural, and Behavioral Physiology* 186, 1073–1087.

Fox, G. L., Coyle-Thompson, C. A., Bellinger, P. F. and Cohen, R. W. (2007). Phototactic Responses to Ultraviolet and White Light in Various Species of Collembola, Including the Eyeless Species, *Folsomia candida*. *J. Insect Sci.* **7**, 1–12.

Heckman, C. W. (2018). *Ecological strategies of aquatic insects.* Boca Raton: CRC Press, Taylor & Francis Group.

Hopkin, S. P. (1997). *Biology of Springtails (Insecta: Collembola).* Oxford; New York; Tokyo: Oxford University Press.

Horváth, G. and Varjú , D. (1997). Polarization pattern of freshwater habitats recorded by video polarimetry in red, green and blue spectral ranges and its relevance for water detection by aquatic insects. *J. Exp. Biol.* **200**, 1155–1163.

Horváth, G. and Varjú , D. (2004). *Polarized Light in Animal Vision – Polarization Patterns in Nature*. Heidelberg; Berlin; New York: Springer.

Horváth, G., Majer, J., Horváth, L., Szivák, I. and Kriska, G. (2008). Ventral polarization vision in tabanids: horseflies and deerflies (Diptera: Tabanidae) are attracted to horizontally polarized light. *Naturwissenschaften* **95**, 1093–1100.

Johnsen, S. (2012). *The Optics of Life.* Princeton, NJ: Princeton University Press.

Mazza, C. A., Izaguirre, M. M., Curiale, J. and Ballare, C. L. (2010). A look into the invisible: ultraviolet-B sensitivity in an insect (Caliothrips phaseoli) revealed through a behavioural action spectrum. *Proc. R. Soc. Biol. Sci. Ser. B* **277**, 367–373.

Menzel, R., and Backhaus, W. (1991). Colour vision in insects, In *The perception of colour, Vol. 6, vision and visual dysfunction* (ed. P. Gouras), pp. 262–293. London: Macmillan.

Noble-Nesbitt, J. (1963). A site of water and ionic exchange with the medium in *Podura aquatica* L. (Collembola, Isotomidae). *J. Exp. Biol.* **40**, 701–711.

Rusek, J. (1998). Biodiversity of Collembola and their functional role in the ecosystem. *Biodiv. Conserv.* **7**, 1207-1219.

Salmon, S. and Ponge, J. F. (1998). Responses to light in a soil-dwelling springtail. *Eur. J. Soil Biol.* **34**, 199–201.

Schwind, R. (1983). A polarization-sensitive response of the flying water bug *Notonecta glauca* to UV light. *J. Comp. Physiol. A* **150**, 87–91.

Schwind, R. (1984). Evidence for true polarization vision based on a two-channel analyzer system in the eye of the water bug, *Notonecta glauca*. *J. Comp. Physiol. A* **154**, 53–57.

Schwind, R. (1989). A variety of insects are attracted to water by reflected polarized light. *Naturwissenschaften* **76**, 377–378.

Schwind, R. (1991). Polarization vision in water insects and insects living on a moist substrate. *J. Comp. Physiol. A* **169**, 531–540.

Schwind, R. (1995). Spectral regions in which aquatic insects see reflected polarized light. *J. Comp. Physiol. A* **177**, 439–448.

Shaller, F. (1972). Observations on the visual reactions of Collembola. In *Information Processing in the Visual Systems of Arthopods* (ed. R. Wehner), pp. 249–253. Heidelberg; Berlin; New York: Springer.

Verheijen, F. J. and Brouwer, J. M. M. (1971). Orientation of Podura aquatica (L.)(Collembola, Insecta) in a natural angular radiance distribution. *Neth. J. Zool.* **22**, 72–80.

Wildermuth, H. (1998). Dragonflies recognize the water of rendezvous andoviposition sites by horizontally polarized light: a behavioural field test. *Naturwissenschaften* **85**, 297–302.

Table

Table 1: Optical characteristics of polarized stimuli in experiment 2 as a function of wavelength. I_{pol}: Relative light intensity compared to the corresponding unpolarized stimulus due to the wavelength dependent transmission of the polarizer. d: degree of polarization $\pm$ standard deviation. $\lambda = 744$ nm was not measurable with our polarimeter.

λ [nm]	I_{pol} [%]	d [%]
421	32.7	93.7 ± 2.1
442	38.7	94.2 ± 2.0
467	41.3	95.6 ± 2.0
496	43.1	95.5 ± 2.1
516	43.7	94.0 ± 2.2
552	44.5	94.4 ± 2.1
598	44.6	93.9 ± 2.5
623	44.7	95.2 ± 2.7
641	44.7	94.0 ± 2.6
660	44.8	94.1 ± 2.7
744	46.7	-

Figures
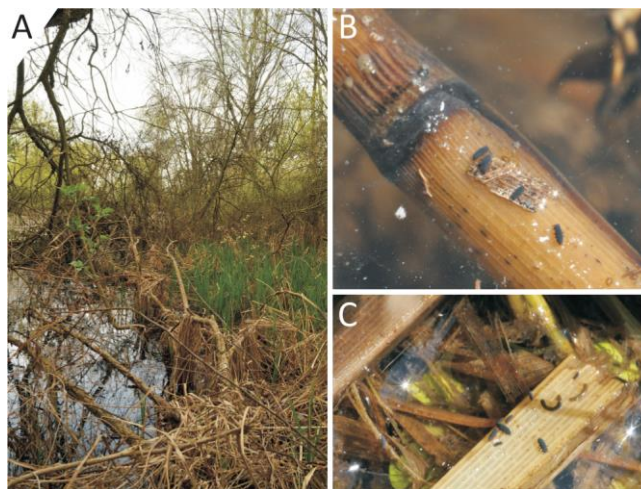
Figure 1: Habitats of *P. aquatica*. (A) One of the sites where springtails were collected during spring. (B-C) *P. aquatica* resting on decaying plant material.
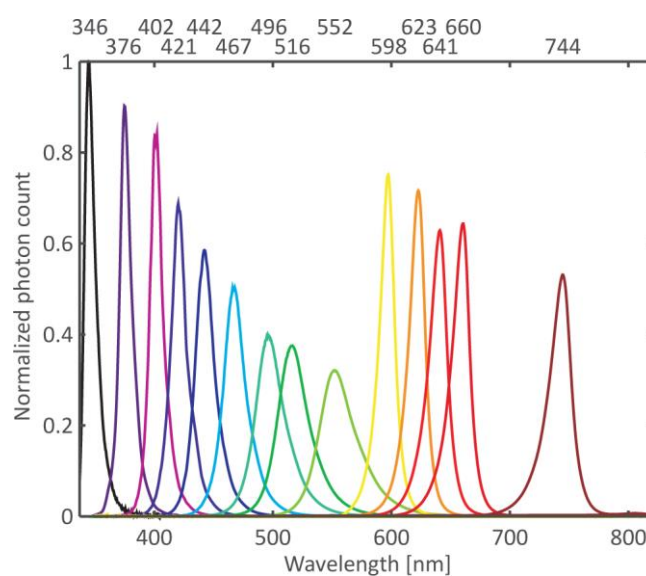
Figure 2: Emission spectra of the monochromatic light stimuli in case of equal photon flux for each LED. Areas under curves are equal. Numbers at the top show the peak wavelengths of the LEDs.
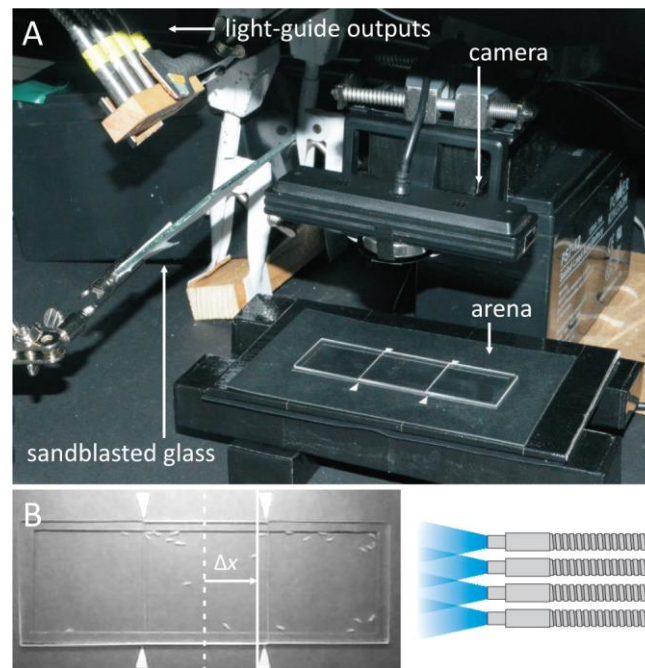
Figure 3: Measurement of the action spectrum of phototaxis. (A) Photograph of the experimental setup. (B) Example image of the camera during a light stimulus of $\lambda_{stimulus} = 442$ nm. The dashed and solid lines represent the horizontal position of the arena center and the centroid of springtails needed for the calculation of Δx.
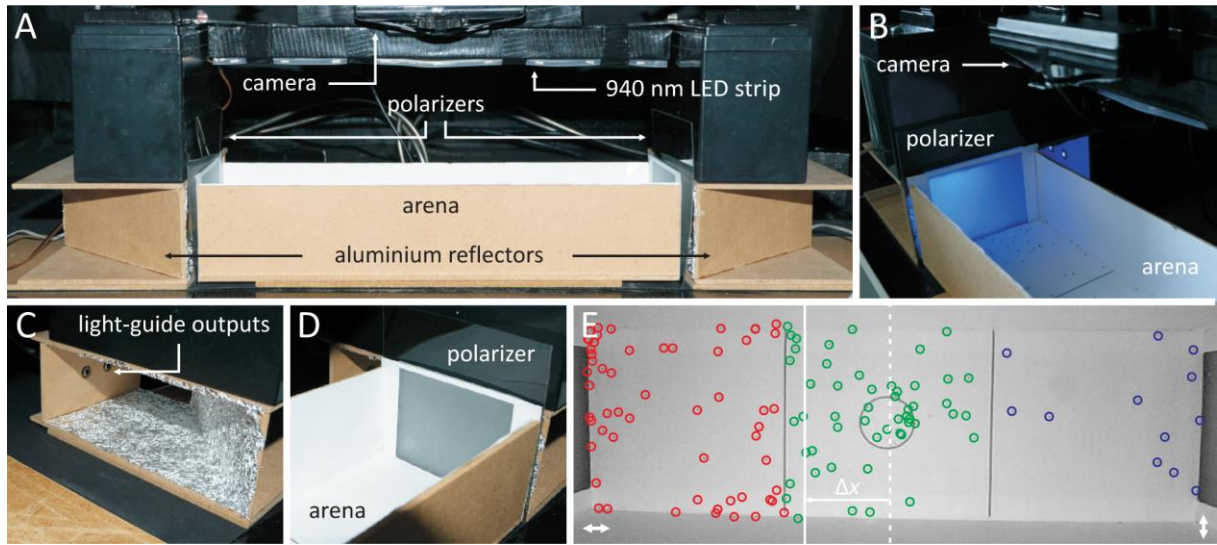
Figure 4: Measurement of the wavelength dependence of polarotaxis. (A) Photograph of the experimental setup. (B) Photograph of the setup with a horizontally polarized blue stimulus ($\lambda_{stimulus}$ = 442 nm). (C) Photograph of the aluminium reflector meant to diffusely reflect light of the light-guide outputs. (D) Same as C, with the arena at normal position. (E) Example for the detection of springtails for a horizontally/vertically (left/right) polarized stimulus pair in experiment 2 (t = 70 s, $\lambda_{stimulus}$ = 496 nm). Relative centroid shift of springails Δx towards horizontally polarized stimulus is calculated as in Fig 3B.
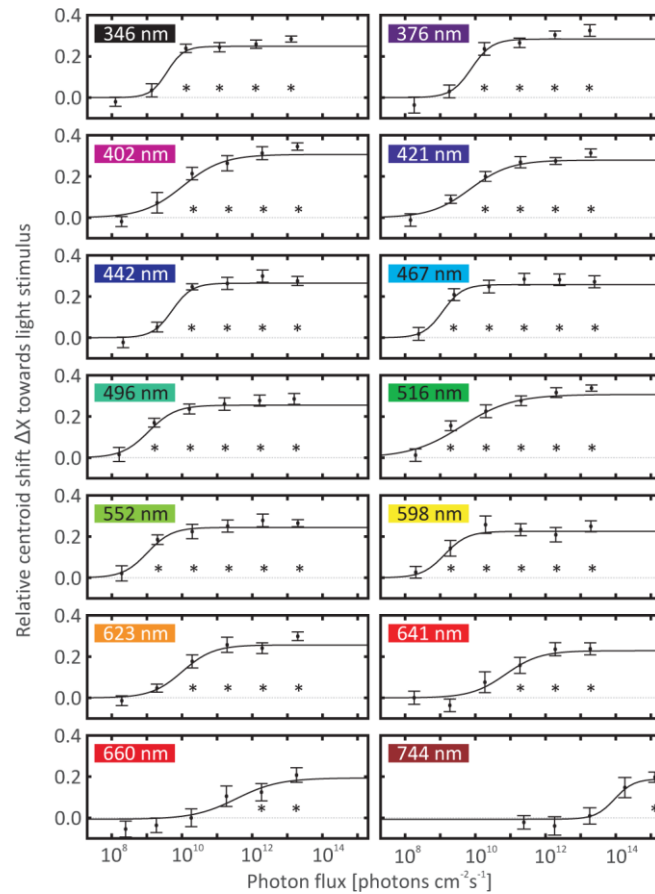
Figure 5: Phototactic responses of *P. aquatica* as a function of photon flux for 14 different wavelengths. Points represent the means of 10 trials ± 1 SE, while solid lines are the fitted sigmoid dose-response curves (Eqn 1). Asterisks display the significance of Mann-Whitney U tests (p < 0.05).
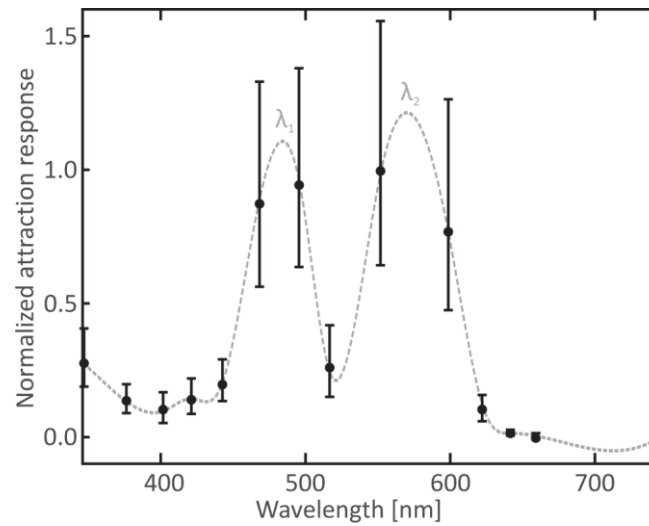
Figure 6: Action spectrum of phototaxis of *P. aquatica*. Vertical bars were calculated from the asymptotic standard errors of log photon flux ($J_{50\%}$) needed for eliciting 50% response, and the dashed line shows cubic spline interpolation. $\lambda_1 = 484$ nm and $\lambda_2 = 570$ nm are the positions of the two maxima.
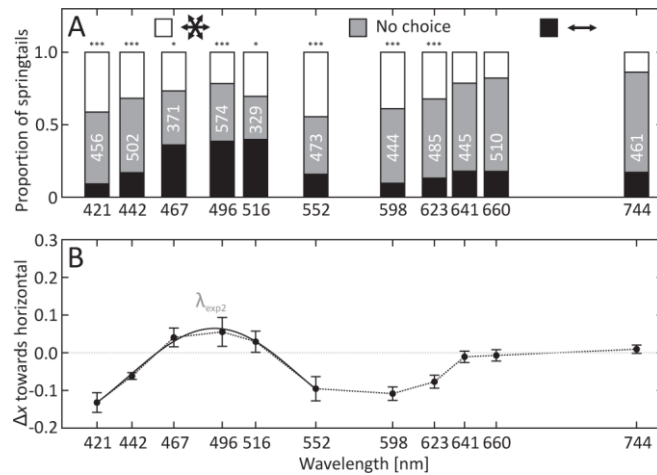
Figure 7: Responses of springtails to horizontally polarized light against unpolarized stimulus as a function of wavelength in experiment 2. (A) Proportion of total springtails in the arena terminals corresponding to the horizontally polarized stimuli (black bars), unpolarized stimuli (white bars) and the inactive specimens in the middle of the arena (grey bars). Total numbers of tested springtails are show in the grey bars. *$p < 0.05$, **$p < 0.001$, ***$p < 0.0001$, in χ^2 tests (B) Mean relative centroid shifts Δx of springtails towards horizontally polarized stimulus. Vertical bars represent the standard errors of the 4 trials. Gaussian function fitted on the 421 nm – 552 nm region is shown by solid line. Wavelength of Gaussian maximum is $\lambda_{exp2} = 491$ nm.
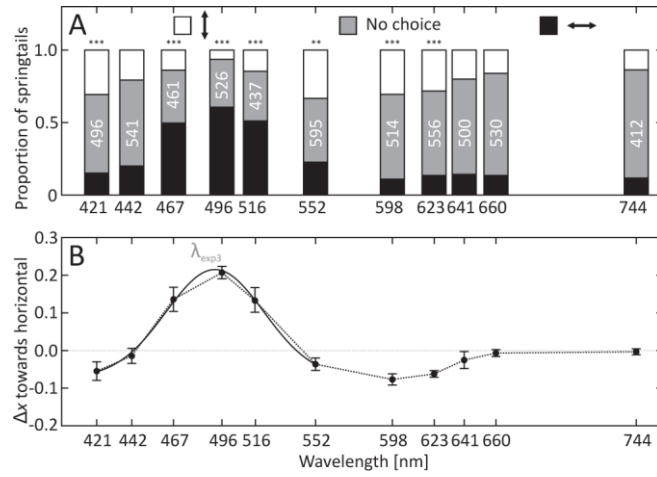
Figure 8: Same as Fig. 7 for equal-intensity stimulus pairs of horizontally and vertically polarized light in experiment 3. Wavelength of Gaussian maximum is $\lambda_{exp3} = 492$ nm.
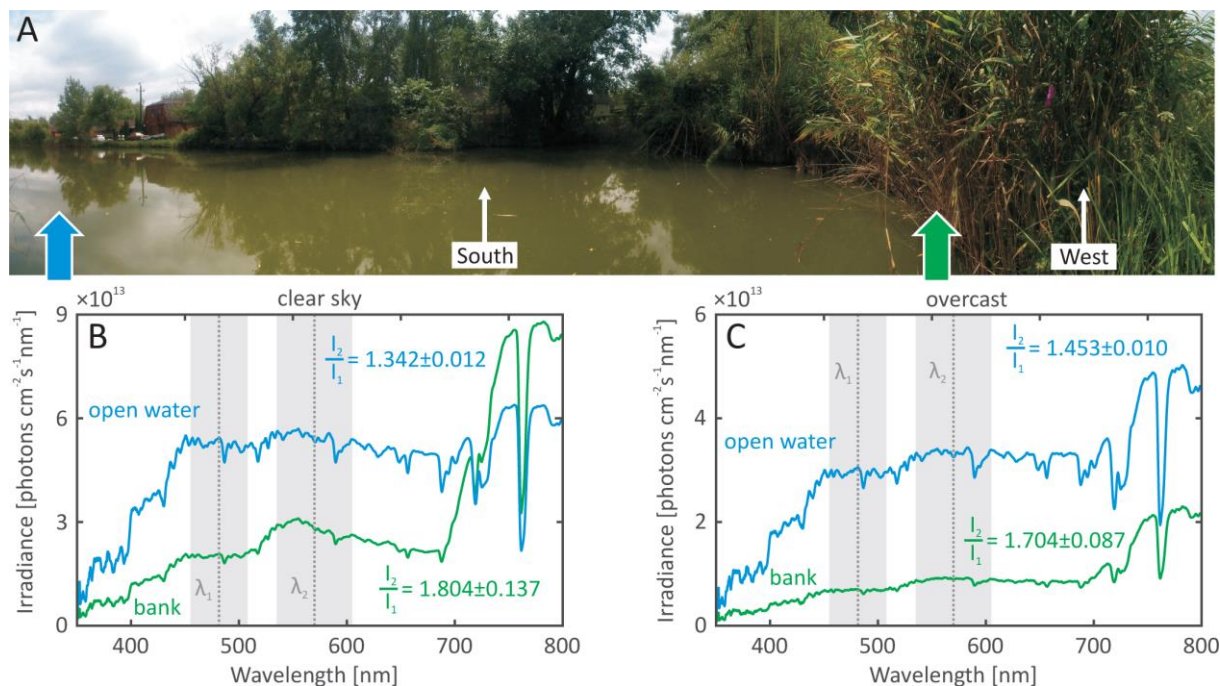
Figure 9: Spectral characteristics of a natural habitat of *P. aquatica*. (A) Panorama photo of a small lake from a fishing pier. The arrows represent horizontal measuring directions (blue: towards open water; green: towards bank). (B) Measured spectrum of the sunny environment with spectrometer directed towards the open water (blue) and the bank (green). Grey regions show the FWHM of the two peaks of the action spectrum of phototaxis (Fig. 6). Mean ratios of integrated photon counts (± SD) in the regions around λ_1 and λ_2 are shown with blue (open water) and green (bank) formulas. (C) Same as B under total overcast conditions.
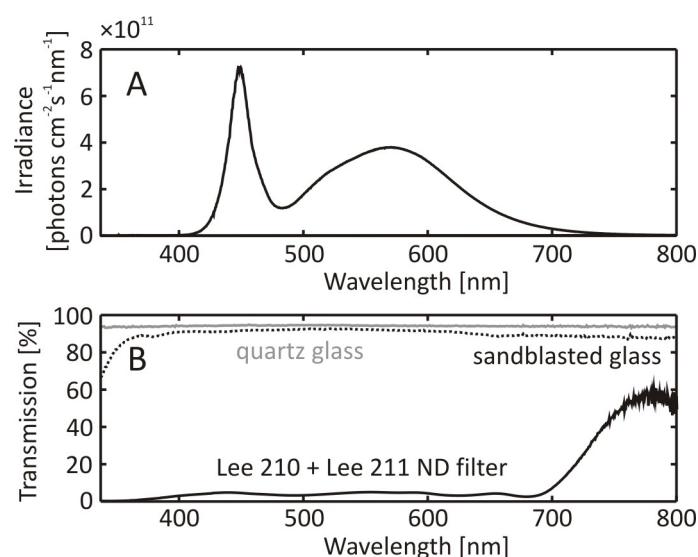
Figure S1. Emission and transmission spectra of components in our project. (A) Emission spectrum of the cool white LED used for lighting the containers with field-caught *P. aquatica*. Cosine corrector of spectrometer was placed at the place of the containers. Total photon flux (area under curve) was 1.47×10^{14} photons·cm^{-2}·s^{-1}. (B) Transmision spectrum of one pair of Lee 210 and Lee 211 neutral density filters (black line), the 3 mm sandblasted glass (dotted line) and the 1 mm quartz glass (grey line).
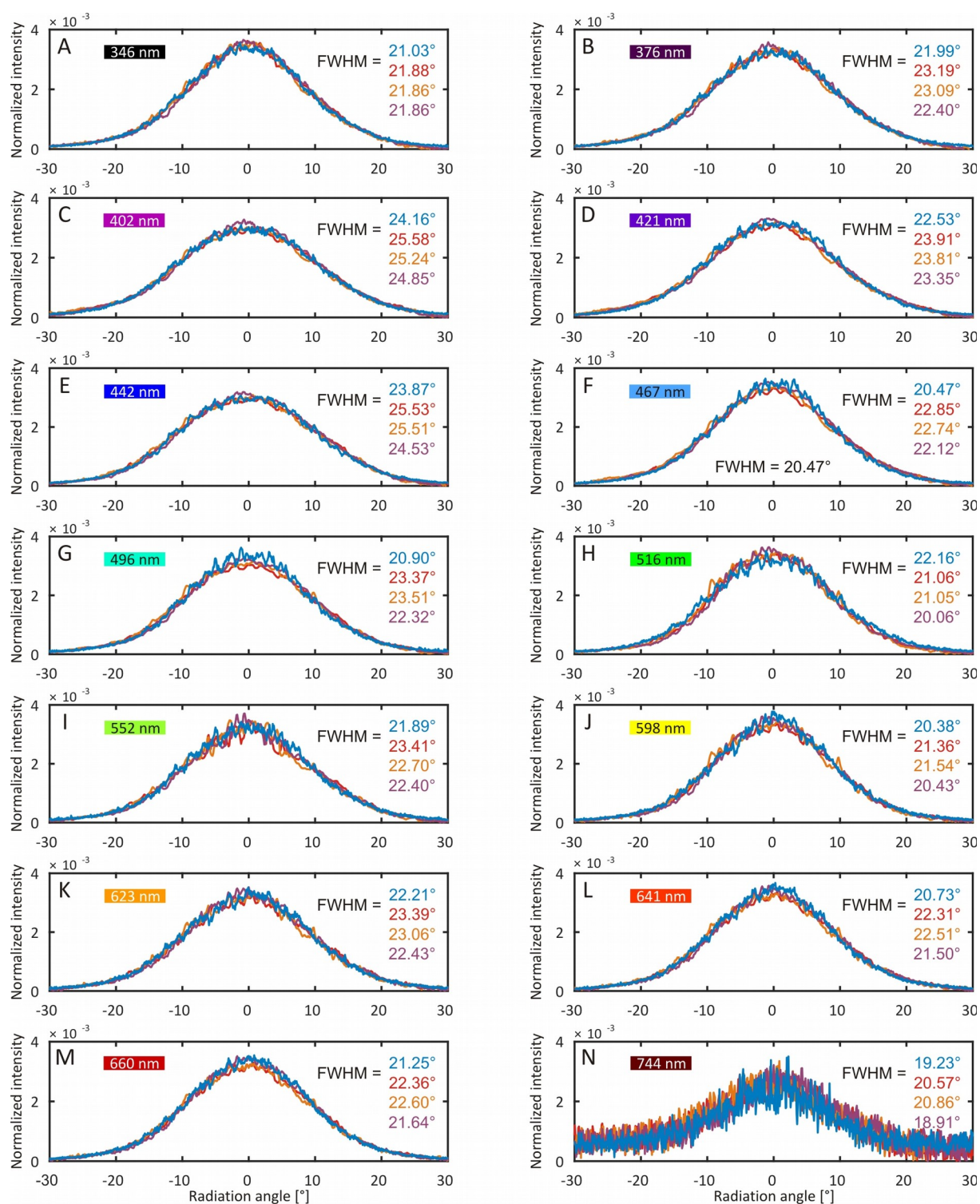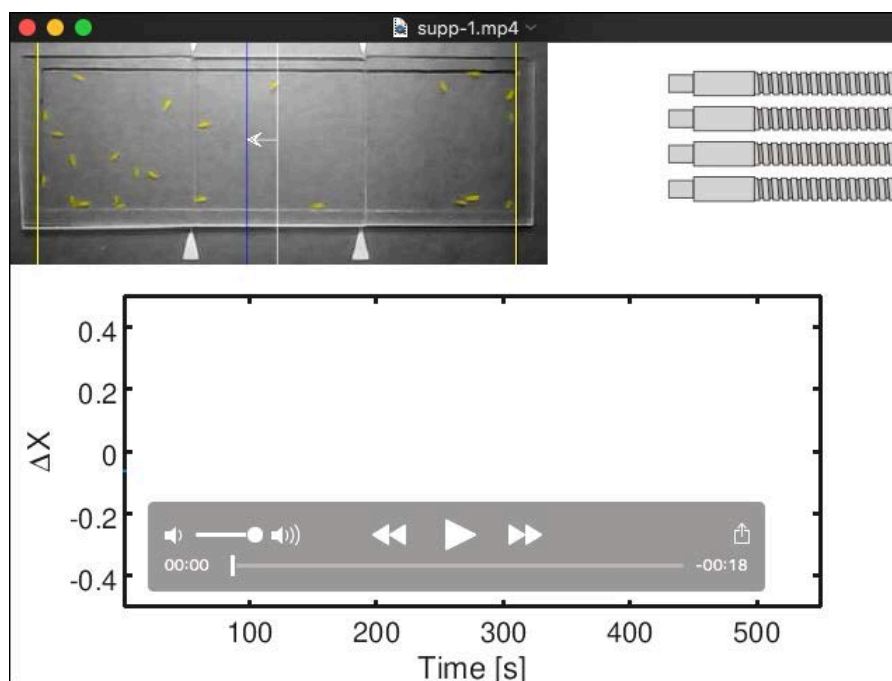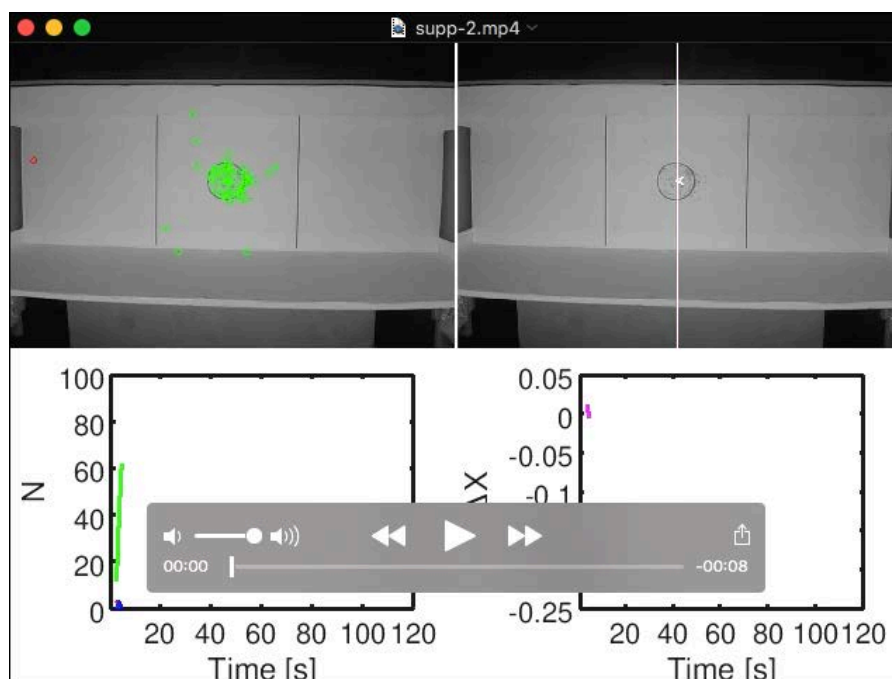
Figure S2. Normalized intensity of light exiting the light-guide outputs measured as a function of angle for all 14 wavelengths. Full-width half-maximum of fitted Gaussian curves are also displayed.

Movie 1. A short demonstration of the trials and data evaluation of experiment 1 for a λ$_{stimulus}$ = 442 nm stimulus.

Movie 2. Evaluation method for the trials of experiments 2 and 3. This example shows a trial when a 100% horizontally (left) and 100% vertically (right) polarized stimulus pair was applied.